

## Probing charge-density-wave dynamics: Spatial noise correlations and nonlocal conduction

S. G. Lemay,\* K. Cicak, K. O'Neill, and R. E. Thorne

Laboratory of Atomic and Solid State Physics, Clark Hall, Cornell University, Ithaca, New York, 14853-2501

(Received 26 March 2001; published 31 October 2001)

We have measured the spatial correlations of low-frequency noise produced by charge-density-wave (CDW) motion in NbSe<sub>3</sub>. The equal-time correlation function is approximately independent of spatial separation up to at least 500 μm, but can change abruptly at macroscopic crystal defects. The nonlocal response of the depinned CDW extends hundreds of μm from a locally applied ac drive and shows current-dependent structure mirroring that observed in the low-frequency noise. These results demonstrate a potentially powerful approach for characterizing CDW dynamics.

DOI: 10.1103/PhysRevB.64.205106

PACS number(s): 71.45.Lr, 72.15.Nj, 72.70.+m, 74.40.+k

The microscopic dynamics that underlies collective charge transport in charge-density-wave (CDW) conductors remains poorly understood.<sup>1</sup> For example, despite a wealth of predictions for field- and frequency-dependent spatial correlations that diverge at dynamical transitions,<sup>2</sup> no experiments have directly probed them. The most detailed information about microscopic dynamics has been provided by measurements of the low-frequency or “broadband” noise (BBN) and of the high frequency coherent oscillations or “narrow-band noise” (NBN), hallmarks of CDW transport.<sup>1,3,4</sup>

The broadband noise produced when the CDW moves has a spectral density  $S(f) \propto f^{-\alpha}$ , where  $\alpha$  is typically 0.8–1.2,<sup>4–6</sup> and an amplitude several orders of magnitude larger than that of the  $1/f$  noise in ordinary metals. Broadband noise is produced by many mechanisms including shear plasticity,<sup>7</sup> plasticity associated with CDW phase slip and current conversion near current contacts and defects,<sup>8–11</sup> and simple thermal activation between metastable states. As with the low-frequency noise that accompanies the motion of flux line lattices in superconductors,<sup>12</sup> the spectral density often exhibits a complicated driving force dependence with sharp, reproducible spikes occurring at particular drives.<sup>13</sup> In large samples the noise is Gaussian, but in small NbSe<sub>3</sub> and *o*-TaS<sub>3</sub> samples individual multilevel fluctuators can be resolved.<sup>14,15</sup> Analysis of these fluctuations suggests that their longitudinal coherence length could exceed 200 μm in small *o*-TaS<sub>3</sub> specimens,<sup>16</sup> and similar values are expected for NbSe<sub>3</sub>.<sup>15,16</sup> These lengths are comparable to those for the NbSe<sub>3</sub> nonlocal response to locally applied current pulses.<sup>17</sup>

Here we describe experiments that attempt to directly probe spatial correlations in CDW dynamics. Using simultaneous measurements of the low-frequency noise in different longitudinal regions of a NbSe<sub>3</sub> whisker the spatiotemporal correlation function of the noise can be evaluated. Some aspects of the low-frequency noise are mirrored in the CDW’s nonlocal response to an externally applied perturbation. Our approach should provide a powerful probe of CDW dynamics.

Noise correlations and nonlocal CDW response were characterized in four nominally pure whiskerlike crystals of NbSe<sub>3</sub> with  $r_R > 300$  and typical cross-sectional dimensions of  $2 \times 10 \mu\text{m}^2$ . These whiskers were mounted onto arrays of 2-μm-wide gold-topped chromium wires as described in

Ref. 18. A dc current  $I_{tot}$  was injected between contacts separated by 5.8 mm. Voltage measurements were performed in the middle region of the whisker more than 2.5 mm from the current contacts, so as to minimize effects of phase slip near the current contacts.

For BBN experiments, voltages  $V_1(t)$  and  $V_2(t)$  were simultaneously measured across two sample segments with lengths of 70 μm and separations varying from 140 to 560 μm, as shown in Fig. 1(a). The voltage cross-correlation function

$$C_{\Delta t}(l) = \frac{\langle V_1(t + \Delta t)V_2(t) \rangle - \langle V_1 \rangle \langle V_2 \rangle}{\sqrt{\langle V_1^2 \rangle - \langle V_1 \rangle^2} \sqrt{\langle V_2^2 \rangle - \langle V_2 \rangle^2}} \quad (1)$$

was then calculated, where  $\langle \rangle$  indicates a time average. Most measurements were performed at  $T = 70$  K on the  $T_{P_1} = 145$  K CDW in NbSe<sub>3</sub>.

For nonlocal ac conduction measurements,<sup>17,19</sup> a small ( $\ll I_T$ ) ac current  $I_{pert}(\omega)$  was applied to one 70 μm segment of the sample and the resulting ac voltage  $V_{resp}(l, \omega)$  across another 70 μm segment a distance  $l$  away was measured using a PAR 5210 lock-in amplifier, as illustrated in

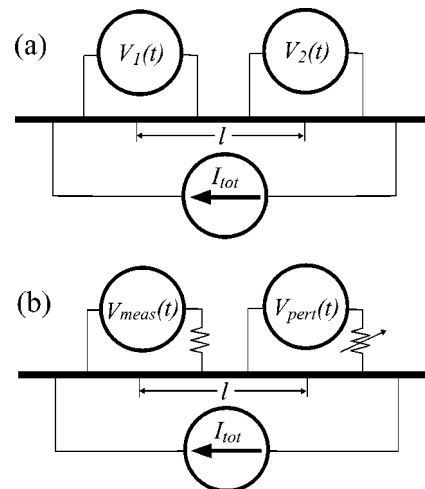


FIG. 1. Measurement geometry for (a) broadband noise correlation measurements and (b) nonlocal conduction measurements. In both cases a dc current is injected through the outermost contacts at either end of the sample.

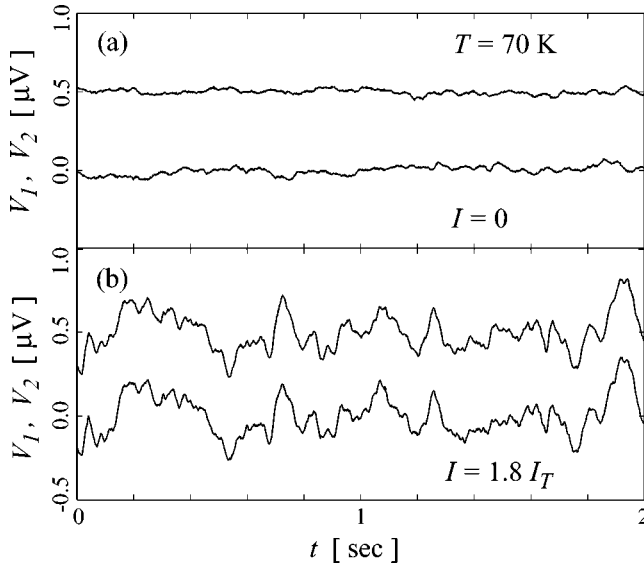


FIG. 2. Simultaneous time traces of voltages within a 1–10 Hz bandwidth across two segments of sample 1 for (a) pinned and (b) sliding states. The corresponding correlation coefficients are  $C_0 = 0.02$  and  $0.94$ , respectively. The two segments were  $70 \mu\text{m}$  long and their centers were  $280 \mu\text{m}$  apart.

Fig. 1(b). Because of the effects of parasitic impedances, measurements were limited to frequencies below 10 kHz.<sup>20</sup>

Figure 2 shows time traces of noise voltages simultaneously recorded across two segments of sample 1 and demonstrates the high degree of correlation that can be exhibited by BBN in the sliding CDW state. Figure 3 shows the equal-time correlation coefficient  $C_0$  as a function of bias current  $I_{tot}$ . The degree of correlation increases sharply from near zero below the CDW depinning threshold  $I_T \approx 290 \mu\text{A}$  to a maximum just above threshold and then slowly decays with further increases in current. Some samples also showed sharp

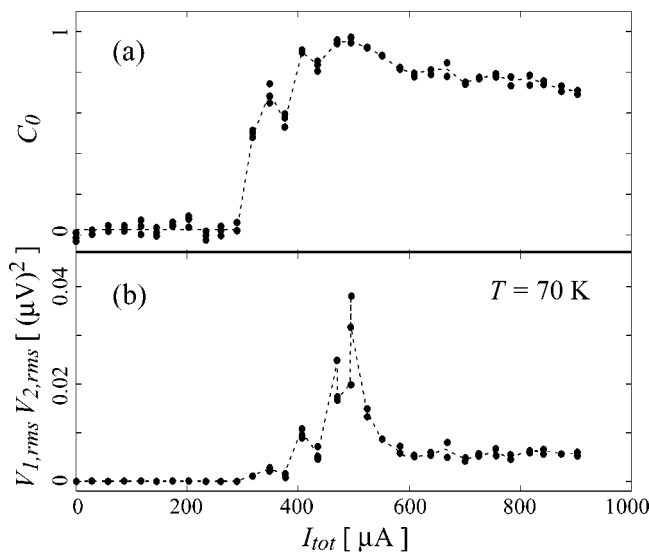


FIG. 3. (a) Correlation coefficient  $C_0$  and (b) product of the rms noise voltage vs driving current  $I_{tot}$  for two  $70 \mu\text{m}$  segments separated by  $l = 280 \mu\text{m}$  in sample 1. The measurement bandwidth is 1–10 Hz. The dotted lines are guides to the eye.

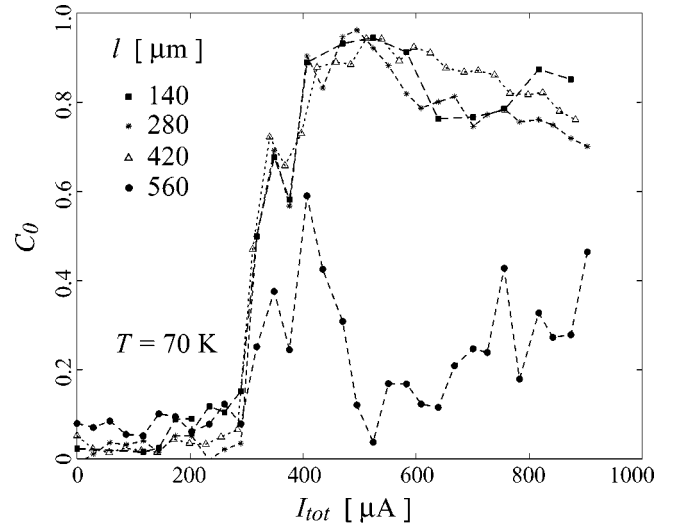


FIG. 4. Correlation coefficient  $C_0$  vs  $I_{tot}$  for four distances  $l$  in sample 1.  $C_0$  is essentially independent of  $l$  until a specific location in the sample is reached, at which points it sharply drops.

spikes in  $C_0$  versus  $I_{tot}$  for  $I_{tot}$  just above  $I_T$ . In all cases studied,  $C_{\Delta t}$  was largest for  $\Delta t = 0$ , placing an upper bound of 0.1 ms on the delay for BBN propagation between segments.<sup>21</sup> Consistent with bulk BBN measurements,<sup>3–6</sup> the product of the rms noise voltages  $v_{1,rms}v_{2,rms}$  increases abruptly at  $I_T$  and shows a spikey maximum just above  $I_T$  before decreasing at larger currents. The maximum of this noise amplitude product corresponds roughly with that of the correlation coefficient.

Figure 4 shows how  $C_0$  for sample 1 depends on the distance  $l$  between segments.  $C_0$  is essentially independent of  $l$ , except for the  $l = 560 \mu\text{m}$  trace where  $C_0$  is much smaller. Some samples showed large correlations up to  $2000 \mu\text{m}$  away, while others showed a loss of correlations on much shorter length scales and/or negative values of  $C_0$ . From this we conclude that the loss of correlation in Fig. 4 is due to a macroscopic sample defect, not to an intrinsic process. The temperature dependence of the correlations has not been studied in detail, but preliminary results indicate that  $C_0$  decreases with increasing temperature: at 120 K in sample 2,  $C_0 < 1\%$  was observed for  $l$  as short as  $140 \mu\text{m}$ . The  $C_\omega$  frequency dependence has also not been studied in detail, but measurements on sample 2 at  $\sim 400$  Hz and  $\sim 4$  Hz gave essentially identical results, consistent with the correlation length being comparable to the sample size.

Figures 5 and 6 show the nonlocal response of samples 2 and 1, respectively, to an applied ac drive. The transfer function  $G(l, \omega) = V_{meas}(l, \omega) / V_{pert}(\omega)$  increases sharply at  $I_T$  and shows a weaker variation at larger  $I_{tot}$ . For sample 1 at fixed  $I_{tot}$ ,  $G(l, \omega)$  decreases on a length scale of hundreds of  $\mu\text{m}$  and shows a somewhat larger decrease for  $l = 560 \mu\text{m}$ . This behavior is roughly consistent with the behavior of  $C_0$ . A characteristic length of hundreds of  $\mu\text{m}$  is also consistent with previous measurements of the nonlocal response to current pulses.<sup>17</sup> Many samples exhibit sharp spikes just above  $I_T$  at biases that correspond to the spikes observed in the noise power versus  $I_{tot}$ .  $G(I_{tot})$  is independent of  $V_{pert}$  (i.e.,

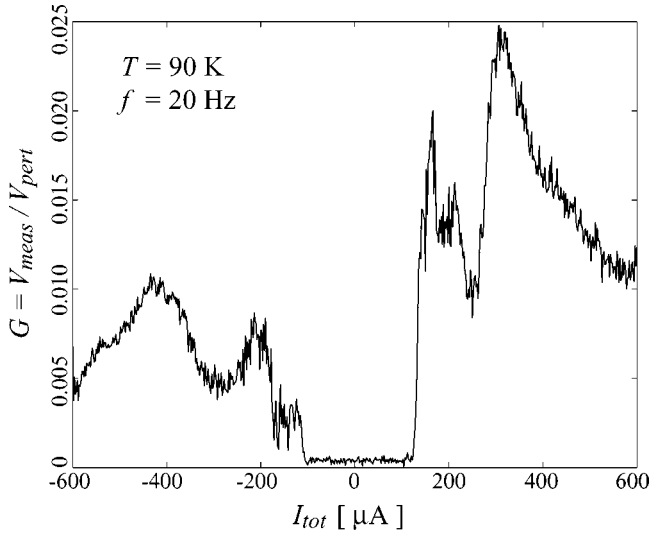


FIG. 5. Transfer function for nonlocal conduction  $G(I_{tot}) = V_{meas}/V_{pert}$  vs  $I_{tot}$  in sample 2, for two segments separated by  $l = 315 \mu\text{m}$ . Nonlocal conduction turns on sharply at threshold and exhibits sharp, sample-dependent spikes that diminish well above threshold. The small signal for  $I_{tot} < I_T$  is due to leakage currents.

$V_{meas}$  varies linearly with  $V_{pert}$  for  $V_{pert} < R_{seg}I_T$ , where  $R_{seg}I_T$  roughly corresponds to the separation of the spikes in  $V_{pert}$ .  $G(I_{tot})$  is usually asymmetric, being larger by about 50% when  $V_{pert}$  is applied to a segment that is at a higher dc voltage than the segment where  $V_{meas}$  is measured.

The amplitude and phase of  $G(\omega)$  are independent of frequency below 10 kHz, the maximum frequency accessible in our measurements. Preliminary measurements indicate that  $G$  is roughly independent of  $T$  below 100 K; above 100 K it decreases with increasing temperature and in our setup became too small to measure near 130 K. As expected, this roughly follows the temperature dependence of the CDW order parameter. At a given temperature below 100 K, the detailed current dependence of  $G(I_{tot})$  is very sensitive to

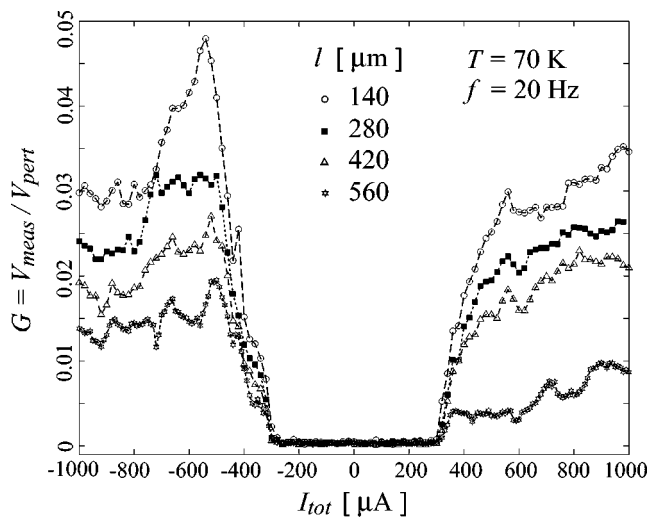


FIG. 6. Transfer function  $G(I_{tot})$  for four segment separations  $l$  for sample 1.

the thermal history of the sample: temperature excursions of the order of 0.1 K are sufficient to cause the peak structure of this curve to change significantly. This behavior is reminiscent of the evolution of the BBN spectrum with temperature cycling.<sup>16</sup>

Our measurements show that the BBN in  $\text{NbSe}_3$  crystals can be  $\sim 95\%$  correlated over distances of hundreds of  $\mu\text{m}$ . Within regions of size  $L$ , the measured noise power scales essentially as  $L^2$ , consistent with the observed correlations. These results confirm the lower bound estimates for the longitudinal BBN coherence length of Refs. 15 and 16, which were based on the amplitude of two-level fluctuators. However, correlations can be destroyed at macroscopic crystal defects that produce discontinuities in the average CDW velocity.

Measurements of the nonlocal ac response show that its bias dependence—especially the very sharp features observed in many samples—closely follows that of the BBN. Below threshold, the CDW is pinned and responds nonlocally only over lengths comparable to the pinning correlation length, on the order of 10  $\mu\text{m}$  in high-purity  $\text{NbSe}_3$ , and so both the BBN amplitude and nonlocal response on  $>100 \mu\text{m}$  lengths are negligible. When the CDW depins, local disturbances can propagate diffusively throughout the CDW over at least hundreds of  $\mu\text{m}$ . The CDW response to a small perturbation should be largest where the dc-driven CDW shows instabilities or abrupt transitions, such as at currents where two-level fluctuators appear and at the low-temperature “switching” threshold.

The dominant sources of BBN in  $\text{NbSe}_3$  are CDW shear occurring along steps in crystal thickness that run along the whisker axis<sup>7</sup> and, in high-quality samples at lower temperatures, current-contact-related phase slip. Shear also causes irregularities in the dc  $I$ - $V$  characteristic. Shear may thus be responsible both for fluctuations in CDW resistance with the dc drive  $I_{tot}$  responsible for the bias-dependent structure in  $G$  and for the local perturbations (likely associated with individual phase slip events) that drive these fluctuations at fixed  $I_{tot}$  to produce BBN.

Additional insight into the present measurements can be obtained by considering a simple one-dimensional model of CDW dynamics.<sup>18</sup> We replace the disordered impurity potential of the Fukuyama-Lee-Rice (FLR) model<sup>1</sup> with a spatially inhomogeneous, time-dependent random force pinning field<sup>22</sup>  $E_p = \bar{E}_p + \delta E_{pert}(x, t)$  to yield an equation of motion for the CDW phase,  $\chi(\rho_c + \rho_n)(\partial\phi/\partial t) = \rho_n j_t - E_p + (\kappa/Q)(\partial^2\phi/\partial x^2)$ . Here  $\chi(\rho_n + \rho_c)$  is a damping constant,  $j_t$  is the dc current density injected at the current contacts,  $\kappa$  is the CDW spring constant,  $Q$  is the CDW wave vector, and  $\rho_n$  and  $\rho_c$  are the quasiparticle and CDW resistivities, respectively. Because of the CDW’s elasticity, a locally applied force can affect CDW motion over large distances. For a fluctuating perturbation  $\delta E_{pert}(x, t) = V_{pert}(t) \delta(x - x_0)$  localized at  $x = x_0$  and with an arbitrary time dependence, the solution for a depinned CDW obtained by linearizing about the steady-state solution for  $\delta E_{pert}(x, t) = 0$  is a diffusion wave.<sup>23</sup> The position- and frequency-dependent electric field induced by the perturbation is, for large  $\omega$ ,

$$\delta E(x, \omega) = -\operatorname{sgn}(x-x_0) \frac{\rho_n}{\rho_n + \rho_c} \sqrt{\frac{\omega}{\omega_0}} \times Q V_{\text{pert}}(\omega) e^{i\pi/4 + (i-1)\sqrt{\omega/2\omega_0} Q|x-x_0|}, \quad (2)$$

where  $\omega_0 = Q\kappa/\chi(\rho_n + \rho_c)$ .

The BBN generated by a localized source at  $x_0$  decays exponentially with distance from  $x_0$ . The frequency-dependent length scale  $\xi_{bbn}(\omega)$  for this decay is, from Eq. (2),  $\xi_{bbn} = Q^{-1}\sqrt{2\omega_0/\omega}$ . This corresponds to a CDW diffusion constant  $D = \omega_0/Q^2$ .

If the BBN is generated by local fluctuators uniformly distributed within the sample, the total BBN amplitude obtained by summing the contributions of individual fluctuators will be independent of position. However, the cross-correlation coefficient  $C(\omega, l) = \langle E_1(\omega)E_2(\omega) \rangle / \langle E_{1,2}(\omega)^2 \rangle$  of the noise sampled at positions  $x_1$  and  $x_2 = x_1 + l$ ,

$$C(\omega, l) = [1 + l/\xi_{bbn}(\omega)] \exp[-l/\xi_{bbn}(\omega)], \quad (3)$$

will decay roughly exponentially with separation  $l$  with a decay length  $\xi_{bbn}$ , reflecting the spatial extent of the individual disturbances.

Within this simple model, Eq. (2) also describes the nonlocal spatiotemporal CDW response to a locally applied external voltage.  $V_{\text{pert}}$  and  $\omega$  then represent the amplitude and frequency, respectively, of a sinusoidal voltage applied longitudinally to a short segment of a crystal.  $\delta E$  is then the nonlocal electric field generated by this perturbation, which also decays on a length  $\xi_{bbn}$ .

Using numbers appropriate for NbSe<sub>3</sub>,<sup>18</sup>  $\xi_{bbn}(\omega) \approx 4$  mm at a frequency of 10 Hz. This correlation length is comparable to the current-contact spacing in our experiments and much greater than the voltage-contact spacing, and is consistent with the noise correlations of Fig. 4 being essen-

tially independent of distance over hundreds of micrometers. However, the model predicts that  $G$  for the nonlocal ac response should also be position independent, but instead a gradual decay is observed in Fig. 6.

Although the simple model provides some insight, its failures are not surprising. First, when  $\xi_{bbn}(\omega)$  is comparable to the distance from  $x_0$  to the current contacts, CDW disturbances caused by a slow perturbation have time to propagate to these contacts and establish a new “equilibrium” CDW current distribution. The form of this distribution depends on the details of the phase slip boundary conditions at the current contacts and on the presence of macroscopic sample defects, neither of which are included. Second, the simple form of the pinning field  $E_p$  ignores the collective dynamics of the CDW interacting with quenched disorder. Third, the model ignores the fact that the measured voltage-current response is due not only to CDW motion, but also to changes in the local single-particle resistivity  $\rho_n(x)$ . At the low frequencies studied here and in Ref. 17, measurements are dominated by the latter contribution.<sup>20,24</sup>

At higher frequencies disturbances will propagate shorter distances on the perturbation’s time scale and contact boundary conditions should become less important. Consequently, an extension of the present measurements to a broader frequency range should permit probing the “intrinsic” spatial correlations in the CDW’s collective dynamics, both near and far from the “washboard” or narrowband noise frequency. An explanation of these correlations is at the heart of all theories of CDW dynamics.

This work was supported by NSF Grant No. DMR97-05433. S.G.L. acknowledges additional support from Canada’s NSERC. Sample holders were prepared at the Cornell Nanofabrication Facility.

\*Present address: Department of Applied Physics, Delft University of Technology, Lorentzweg 1, 2628 CJ Delft, The Netherlands.

<sup>1</sup>See review articles by P. Monceau, G. Grüner, and J. C. Gill, in *Physics and Chemistry of Low-Dimensional Inorganic Conductors*, Vol. 354 of NATO Advanced Study Institute, Series B: Physics, edited by C. Schlenker, M. Greenblatt, J. Dumas, and S. van Smaalen (Plenum, New York, 1996); R.E. Thorne, *Phys. Today* **49**(5), 42 (1996).

<sup>2</sup>D.S. Fisher, *Phys. Rep.* **301**, 113 (1998); L. Balents and M.P.A. Fisher, *Phys. Rev. Lett.* **75**, 4270 (1995); L. Balents, M.C. Marchetti, and L. Radzihovsky, *Phys. Rev. B* **57**, 7705 (1998).

<sup>3</sup>R.M. Fleming and C.C. Grimes, *Phys. Rev. Lett.* **42**, 1423 (1979).

<sup>4</sup>J. Richard, P. Monceau, M. Papoular, and M. Renard, *J. Phys. C* **15**, 7157 (1982).

<sup>5</sup>A. Zettl and G. Grüner, *Solid State Commun.* **46**, 29 (1983).

<sup>6</sup>S. Bhattacharya, J.P. Stokes, M.O. Robbins, and R.A. Klemm, *Phys. Rev. Lett.* **22**, 2453 (1985).

<sup>7</sup>M.P. Maher *et al.*, *Phys. Rev. B* **43**, 9968 (1991); Y. Li *et al.*, *Phys. Rev. Lett.* **83**, 3514 (1999).

<sup>8</sup>J. C. Gill, in *Physics and Chemistry of Low-Dimensional Inorganic Conductors* (Ref. 1), p. 411.

<sup>9</sup>N.P. Ong and K. Maki, *Phys. Rev. B* **32**, 6582 (1985).

<sup>10</sup>P. B. Littlewood, in *Charge Density Waves in Solids*, edited by L.

P. Gor’kov and G. Grüner (North-Holland, Amsterdam, 1989), p. 321.

<sup>11</sup>M. Goldbach, T. Meyer, N. Sandersfeld, and J. Parisi, *Phys. Rev. A* **238**, 179 (1998).

<sup>12</sup>For example, see W.J. Yeh and Y.H. Kao, *Phys. Rev. B* **44**, 360 (1991); A.C. Marley, M.J. Higgins, and S. Bhattacharya, *Phys. Rev. Lett.* **74**, 3029 (1995).

<sup>13</sup>For example, see M.S. Sherwin and A. Zettl, *Phys. Rev. B* **32**, 5536 (1985).

<sup>14</sup>S.V. Zaitsev-Zotov and V.Y. Pokrovskii, *Pis'ma Zh. Éksp. Teor. Fiz.* **49**, 449 (1989) [*Sov. Phys. JETP* **49**, 514 (1989)]; V.Y. Pokrovskii, and S.V. Zaitsev-Zotov, *Europhys. Lett.* **13**, 361 (1990); S.V. Zaitsev-Zotov, V.Y. Pokrovskii, and J.C. Gill, *J. Phys. (Paris)* **2**, 111 (1992).

<sup>15</sup>I. Bloom, A.C. Marley, and M.B. Weissman, *Phys. Rev. Lett.* **71**, 4385 (1993); *Phys. Rev. B* **50**, 12 218 (1994).

<sup>16</sup>A.C. Marley, I. Bloom, and M.B. Weissman, *Phys. Rev. B* **49**, 16 156 (1994); A.C. Marley and M.B. Weissman, *ibid.* **46**, 12 794 (1992).

<sup>17</sup>J.C. Gill, *Europhys. Lett.* **11**, 175 (1990).

<sup>18</sup>T.L. Adelman *et al.*, *Phys. Rev. B* **52**, R5483 (1995).

<sup>19</sup>Several studies of nonlocal effects in dc transport have been re-

ported. For example, see M.C. Saint-Lager, P. Monceau, and M. Renard, *Europhys. Lett.* **9**, 585 (1989).

<sup>20</sup>S. G. Lemay, Ph.D. thesis, Cornell University, 1998.

<sup>21</sup>Propagation delays have been observed in low-frequency, quasi-periodic oscillations in the blue bronzes just above threshold [T. Csiba, G. Kriza, and A. Jánossy, *Phys. Rev. B* **40**, 10 088 (1989)]. These relaxationlike oscillations are distinct in origin

from the BBN studied here.

<sup>22</sup>This assumes that impurities are not the origin of the low-frequency noise, consistent with the  $T=0$  elastic limit of the FLR model.

<sup>23</sup>For a recent review on diffusion waves, see A. Mandelis, *Phys. Today* **53**(8), 29 (2000).

<sup>24</sup>S.G. Lemay *et al.*, *Phys. Rev. B* **57**, 12 781 (1998).